Supporting Information

Eberlin et al. 10.1073/pnas.1215687110

SI Materials and Methods

Sample Collection. All surgeries were performed at BWH, Harvard Medical School. During the course of tumor resection, the surgeon removed small pieces of tissue with tumor forceps or surgical aspirator, and these were labeled to indicate the sample number and position. The stereotactic neuronavigation pointer was used to identify the sample position on preoperative MRI, and the corresponding 3D coordinates were digitally registered for most of the samples obtained. Surgical samples were also obtained using the Cavitron Ultrasound Surgical Aspirator (Integra Radionics). The bulk of the tumor was used for standard histopathological permanent-staining protocols. During or immediately after surgery, the samples for DESI-MS analysis were flash frozen in liquid nitrogen and stored at −80 °C until sectioned at 10-μm thickness using a Microm HM550 cryostat (Mikron Instruments, Inc.), and thaw-mounted onto glass slides. The slides were stored at −80 °C; and dried in a dessicator before analysis. Meningioma samples were obtained from the BWH Neuro-oncology Program Biorepository collection, and analyzed under approved IRB protocol. Tissue sections were prepared under the same experimental conditions as the above surgical samples.

Histopathology Analysis. Tumor content was evaluated by a neuropathologist through examination of an H&E-stained tissue section, which was adjacent to the one used for DESI-MS imaging studies. Tumor was also evaluated on the diagnostic permanent H&E section for each patient. Specimens were evaluated and scored visually with respect to their percentage of tumor nuclei relative to the total nuclei in the sample. Samples were also characterized and assigned a qualitative score from normal to infiltrative to solid, corresponding from low to high cellularity. MS data interpretation and histopathological evaluation were performed in a blinded fashion at different institutions. Subsequent discussions helped evaluate performance of the MS approach but did not influence results.

DESI Imaging. DESI-MS imaging was performed at Purdue University using methanol:water (1:1 vol/vol) as the solvent system, at a flow rate of 1.5 μL/min, and nitrogen gas pressure of 175 psi. Under the experimental conditions used in this study, the pixel size in the ion images was of 200 × 200 μm^2, although higher or lower spatial resolution can be achieved in DESI-MS imaging. An in-house program allowed the conversion of the XCalibur 2.0 mass spectra files (.raw) into a format compatible with the Biomap software with which spatially accurate images were assembled.

Statistical Analysis—ROI Selection. To create a cancer type classification model, a software tool was developed to enable the selection of regions of interest (ROI) based on visual inspection of the DESI ion image loaded in Biomap so as to maximize the number of pixels that contain molecular information. More specifically, a software tool was developed to draw a rectangle with x, y coordinates over an ion image for selection of ROIs, and the corresponding spectral data are extracted from the ROI, saved in a separate folder, and converted for further analysis using ClinProTools 2.2 (Bruker Daltonics). The entire mass spectrum acquired, from m/z 200 to m/z 1000, was imported into ClinProTools and used for classification. All ROIs were assigned by the neuropathologist for tumor subtype, grade, and cell concentration.

Image-Guided Neurosurgery. The iPlanNet software was also used to fuse all images, segment the targeted resection area, and create 3D models for viewing during surgery; the imaging plan was then transferred to the Cranial 2.1 navigation system. This system was also used to mark the three dimensional locations of tissue samples acquired for the study.

3D Visualization of MRI. To plot the MRI data obtained, 3D Slicer (www.Slicer.org) (version 4.1) (1, 2), an open-source medical imaging visualization tool provided by the National Alliance for Medical Image Computing consortium, was used (3).

3D Visualization of MRI and MS Data. For each glioma classifier, the tabulated classification results were used as weighted input to determine the plotted color as follows. Each of the three classes was assigned to a bin of red, green, or blue (as indicated on the color triangle legend for each figure). The color bin with the greatest number of spectra assigned was set to give 100% contribution of the assigned primary color, and the other bin contributions were weighted based on the maximum.

Statistical Analysis—Comment on Number of Cases and Their Selection. In the present manuscript we describe results obtained for five surgical cases examined by DESI-MS imaging: cases 2, 3, 4, 5, and 8. There were many surgical cases for which samples were collected stereotactically. The cases were de-identified and sequentially numbered for this (and possible future) research projects. From the cases for which samples were available, we selected eight to be analyzed by DESI-MS imaging. Selection was based on cancer diagnosis, as our goal was to examine cases of different diagnosis (astrocytoma, meningioma, oligodendroglioma, etc.) to test the performance of our methodology in recognizing different brain cancer types and grades. From the eight cases analyzed by DESI-MS, we interpreted the results and performed statistical analysis and histopathological evaluation on five chosen randomly (cases 2, 3, 4, 5, and 8)—those discussed in the paper, and for which classification results are shown in Tables 1 and 2. Due to lack of space in the paper, case 5 is discussed in the Supporting Information.

SI Results and Discussion

Surgical Case 2. With DESI-MS analysis, we were able to appropriately classify all of these samples as gliomas (Table 1). It is interesting to note that sample S15, although correctly classified as mostly glioma, presented the poorest agreement, being 73% glioma and 27% meningioma. Histopathological evaluation of the H&E-stained section revealed a fragment of dura and connective tissue admixed with the glioma. This likely contributed to the 27% meningioma designation by our classifier.

Surgical Case 3. All samples were submitted for glioma subtype classification, and all but one specimen were recognized as oligodendroglioma. Sample S21, which contained regions of gray matter, was heterogeneously classified as 43% astrocytoma, 17% oligoastrocytoma, and 40% oligodendroglioma. Samples were also tested by the grade classifier, and correctly classified as WHO grade III. Note for example sample S20, previously discussed for its very characteristic lipid profile, was correctly classified as an oligodendroglioma of 93% grade III. When tumor cell concentration was tested, all samples presented medium to high tumor cell concentration, which also agreed with histopathological evaluation of the H&E-stained tissue sections.

Surgical Case 5. Surgical case 5 consisted of an anaplastic oligodendroglioma case, grade III, recurrent from a previous right parietal oligodendroglioma. The five surgical specimens (S28–S32) obtained from surgery for this case were imaged by DESI-MS in the negative-ion mode. Four specimens were stereotactically registered (samples S29–S32, registered as positions A–D, respectively). The remaining sample (S28) was removed from the bulk of the tumor and also used for diagnosis during neurosurgery using standard histopathological methods. Negative-ion mode mass spectra obtained for sample S28 showed the highly characteristic lipid profile for oligodendroglioma grade III (4). Pathological evaluation of a serial section confirmed that the specimen consisted of a grade III oligodendroglioma, of medium-high tumor cell concentration. Similar mass-spectral results were obtained for samples S29 and S32, for which lipid profiles were indicative of oligodendroglioma with features transitional between grade II and grade III, also confirmed by the neuropathologist as grade II–III oligodendroglioma with medium tumor cell concentration.

DESI-MS mass spectra recorded for the five samples of case 5 were initially tested for brain tumor type, followed by glioma subtype, grade, and tumor cell concentration. Results are reported in Table S2. When tested for brain tumor type, four of the five samples were classified as glioma. It was a surprise that sample S28 was misclassified as meningioma. When the samples were tested for glioma subtype, however, sample S28, as well as samples S29, S30, and S32, were correctly classified as oligodendroglioma, and S31 was classified as astrocytoma. Histopathological evaluation of S31 revealed that the sample presented low-grade features, with low concentrations of tumor cells infiltrating normal brain tissue, which could account for the misclassification. This was consistent with the results for the tumor cell concentration classifier, which correctly indicated S31 as low-medium tumor cell concentration, as well as samples S29, S30, and S32, although S28 presented medium-high tumor cell concentration. It is interesting to note that when tested for grade, samples were classified as mostly containing grade IV features, with the exception of S28, which was classified as 93% grade III. Classification results for the stereotactically registered samples S29–S32 can be visualized in segmented 3D preoperative MRI volume reconstruction of the tumor and surrounding regions, as shown in Fig. S5 for the concentration and grade classifiers.

1. Pieper S, Lorensen B, Schroeder W, Kikinis R (2006) The NA-MIC Kit: ITK, VTK, pipelines, grids and 3D slicer as an open platform for the Medical Image Computing community. *Proceedings of the Third IEEE International Symposium on Biomedical Imaging*, pp 698-701.
2. Pieper S, Halle M, Kikinis R (2004) 3D slicer. *Proceedings of the Second IEEE International Symposium on Biomedical Imaging*, pp 632-635.
3. Talos I-F, Jakab M, Kikinis R, Shenton ME (2008) SPL-PNL Brain Atlas. SPL-PNL Brain Atlas March. Available at http://www.spl.harvard.edu/publications/item/view/1265. Accessed December 20, 2012.
4. Eberlin LS, et al. (2012) Classifying human brain tumors by lipid imaging with mass spectrometry. *Cancer Res* 72(3):645–654.

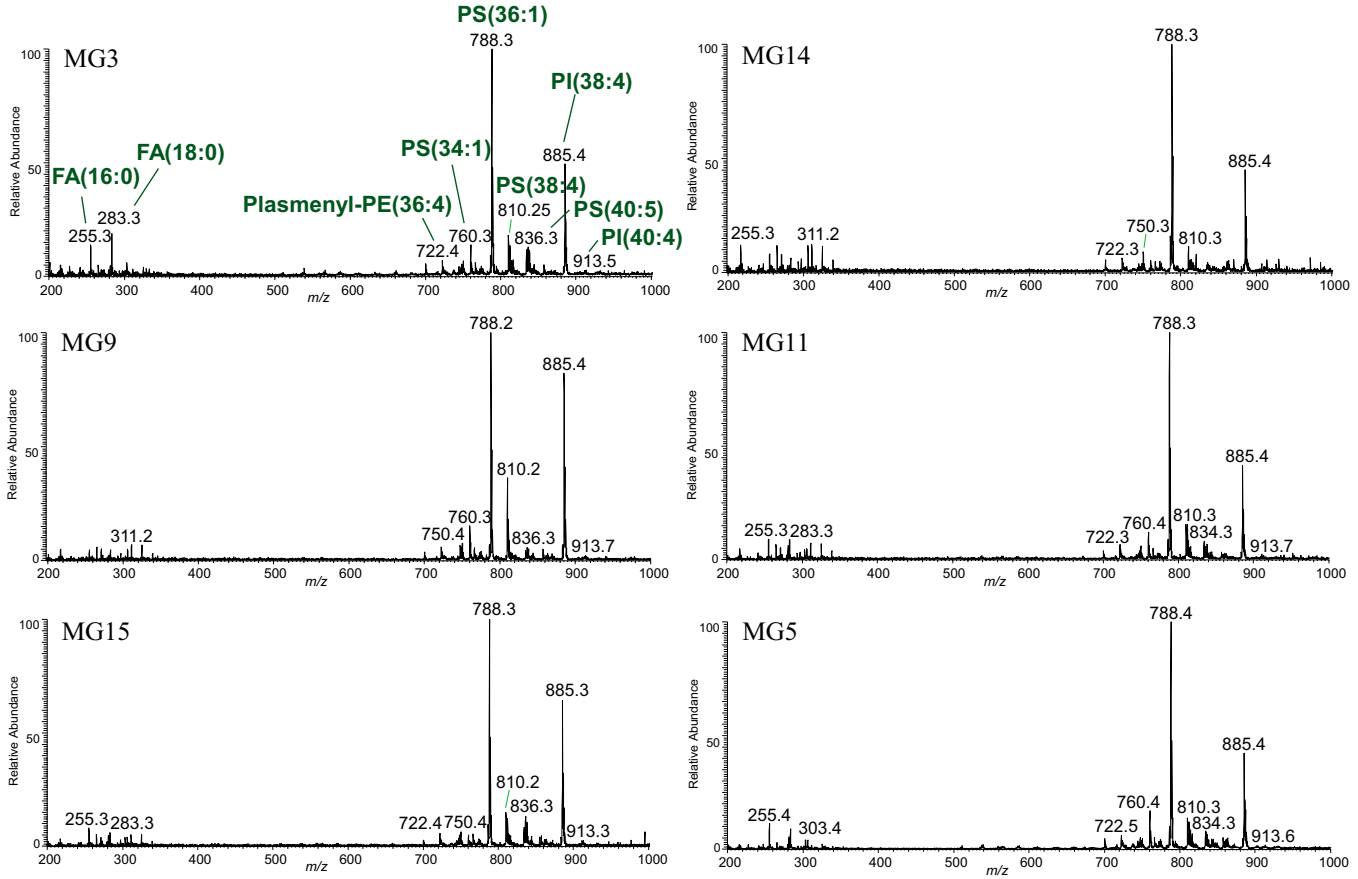

Fig. S1. Negative ion mode DESI-MS mass spectra of six human meningioma specimens, all WHO grade II

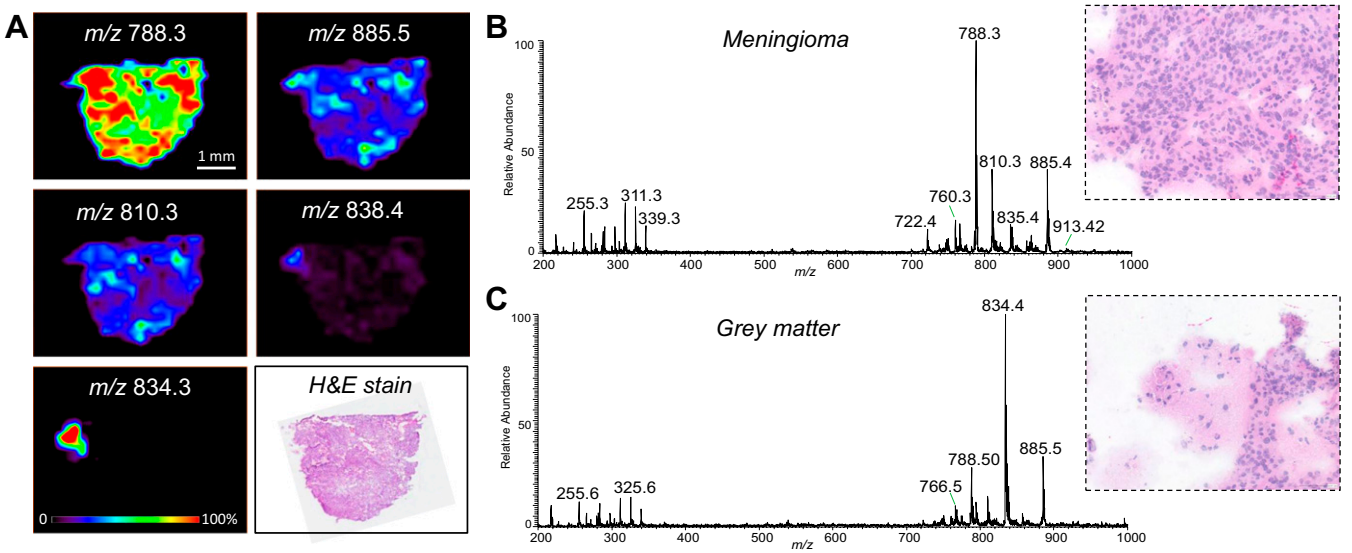

Fig. S2. DESI-MS imaging of meningioma tissue. (*A*) Negative ion mode DESI-MS ion images of MG12, showing the distribution of *m/z* 788.3, *m/z* 885.4, and *m/z* 810.3 (found in higher relative intensities in meningioma region), *m/z* 838.4 and *m/z* 834.4 (found in higher relative intensities in gray matter region). Optical image of an H&E-stained serial section. DESI-MS ion images revealed regions of heterogeneous lipid composition within the tissue section, which were confirmed by pathology to be due to presence of normal gray matter within meningioma tissue. (*B*) DESI-MS mass spectra of meningioma region and (*C*) normal gray matter region of the tissue section.

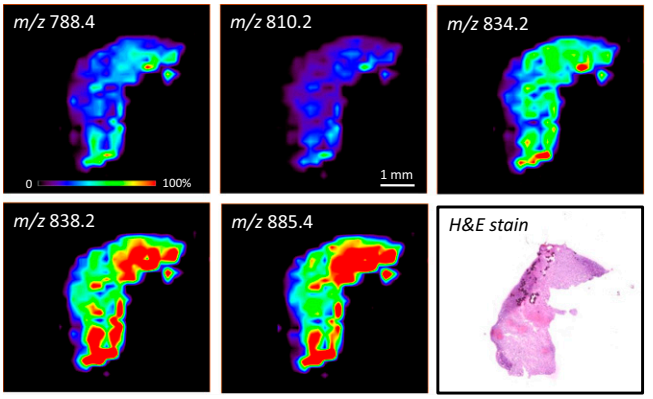

Fig. S3. Negative-mode DESI-MS ion images of sample S20, surgical case 3, showing the distribution of *m/z* 788.4, *m/z* 810.2, *m/z* 834.2, *m/z* 838.2, and *m/z* 885.4. The last image is an optical image of H&E-stained serial section, evaluated by the neuropathologist

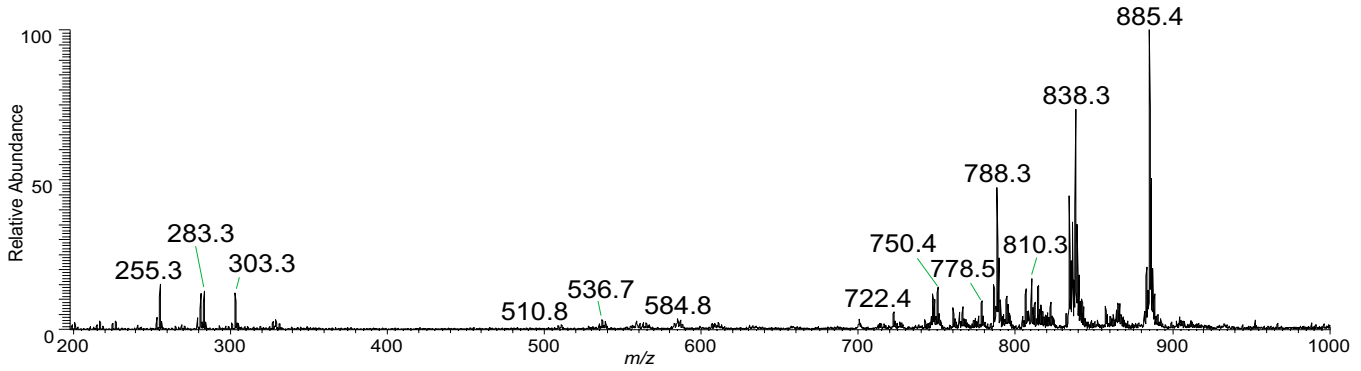

Fig. S4. Representative negative ion mode DESI-MS mass spectra of sample S28, surgical case 5. The lipid profile observed is highly characteristic of glioma of subtype oligodendroglioma and WHO grade III.

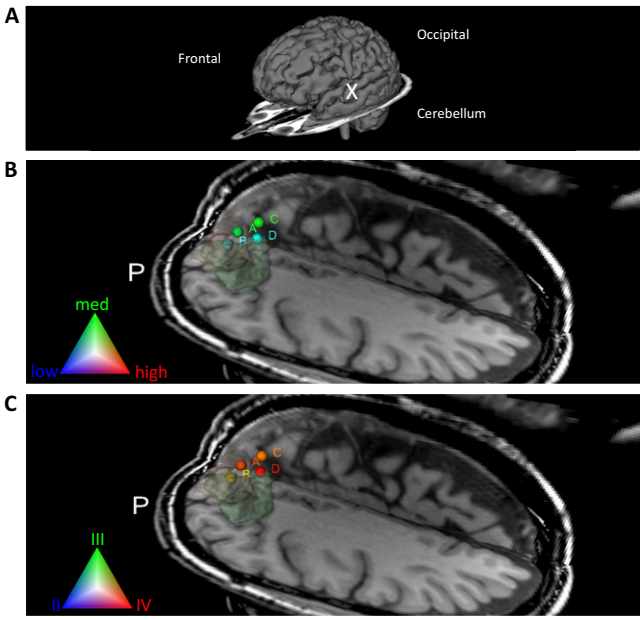

Fig. S5. A schematic of the full brain showing tumor position with an "X" is shown in (*A*). Rendering of tumor cell concentration (*B*) and grade classification (*C*) results for surgical case 5 visualized in segmented preoperative 3D-MRI volume reconstruction of the tumor and surrounding regions. Tumor volume is represented in light green.

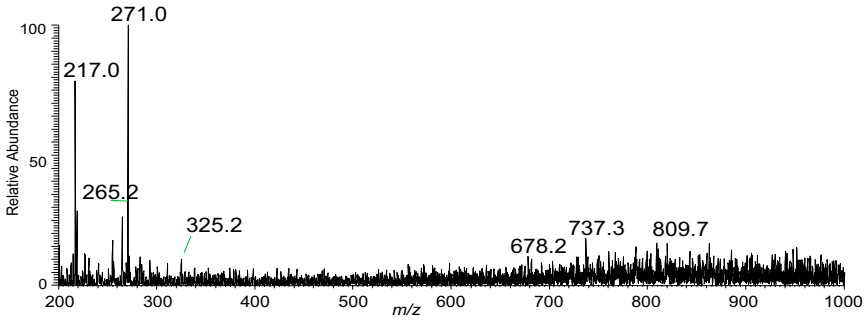

Fig. S6. Representative DESI-MS negative-ion mode mass spectrum of a nonmeningioma region of surgical sample S23 from case 4, meningioma.

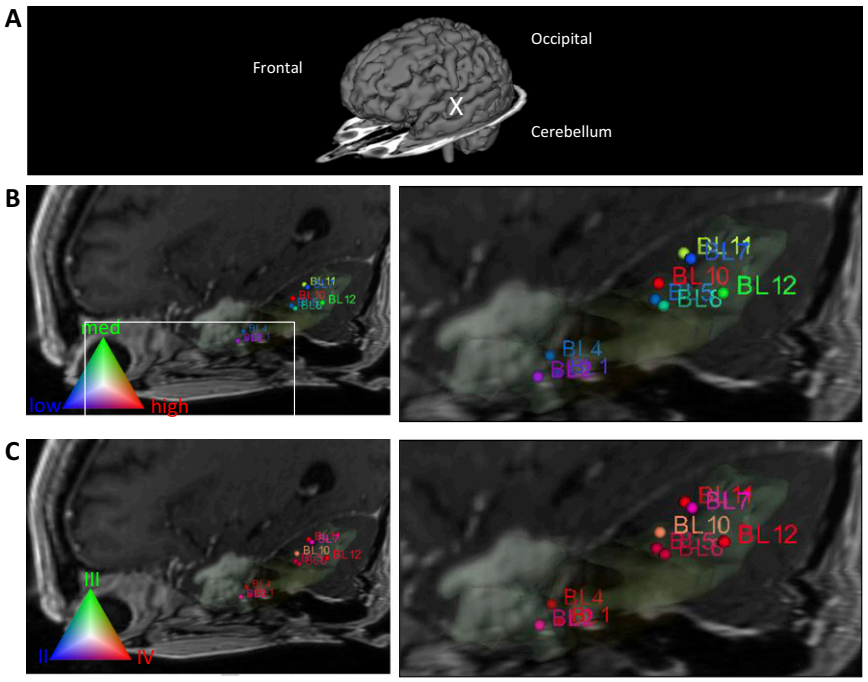

Fig. S7. A schematic of the full brain showing tumor position with an "X" is shown in (*A*). Rendering of tumor cell concentration (*B*) and grade classification (*C*) results for surgical case 8 visualized in segmented preoperative 3D-MRI volume reconstruction of the tumor and surrounding regions. Zoomed in views are shown to the right to facilitate comprehension of the static 3D rendering. Tumor volume is represented in light yellow.

Table S1. Classification results for brain tumor type classifier applied to validation set of samples

		Primary brain cancer type	
Name	WHO diagnosis	Glioma	Meningioma
G_{20}	OA–II; residual A–II; med	100	0
G_{26}	A–IV; recurrent OA–III	100	0
G_{29}	A–IV–O; recurrent OA–III	100	0
G_{30}	A–IV–O; recurrent; high	100	0
G_{32}	A–IV; recurrent A–IV, high	100	0
G_{41_0}	O–II/III; recurrent O–II, high	100	0
G_{46}	A–IV–O; recurrent A–III, high	100	0
G_{47_0}	A–IV–O; recurrent O–II	100	0
G_{47_1}	A–IV–O; recurrent O–II	98	2
G_{48_0}	A–IV; focal gliosarcoma	100	0
G_{49}	O–II; gemistocytes, high	99	1
G_5	A–IV–O; high (80%)	100	0
G_6	A–IV; high	100	0
G_8	A–IV; recurrent A–IV	100	0
MG_{10}	Grade II meningioma	0	100
MG_{12}	Grade II meningioma	1	99
MG_{14}	Grade II meningioma	1	99
MG_{16}	Grade III meningioma	0	100
MG_2	Grade I meningioma	2	98
MG_{20}	Grade II meningioma	0	100
MG_4	Grade I meningioma	0	100
MG_6	Grade I meningioma	8	92
MG_8	Grade II meningioma	0	100

Percentages shown in the table correspond to the percentage of the total number of pixels within the selected ROI classified as glioma or as meningioma. Overall recognition capability is 100%, and cross-validation is 99.7%. Cross-validation (leave-out 20%/10 iterations). A, astrocytoma; OA, oligoastrocytoma; O, oligodendroglioma.

Table S2. Classification results for surgical specimens from surgical case 5

		Tumor type (%)		Glioma subtype (%)			Glioma grade (%)			Glioma concentration (%)		
Name	Diagnosis	GL	MG	A	OA	O	II	III	IV	Low	Med	High
Case 5												
S28	O, III, med	*34*	*66*	12	26	63	0	93	8	4	67	29
S29 (A)	O, III, med	68	32	10	7	83	*1*	*24*	*75*	26	74	0
S30 (C)	O, III, med	84	16	47	0	53	*2*	*33*	*64*	11	78	11
S31 (D)	O, II, low	85	15	*46*	*17*	*38*	*0*	*6*	*94*	*48*	*52*	0
S32 (B)	O, III, med	63	38	35	0	65	3	45	53	43	43	15
Total		56	44	22	15	63	1	57	42	19	65	16